ISSN 1063-7761, Journal of Experimental and Theoretical Physics, 2013, Vol. 117, No. 6, pp. 1032–1041. © Pleiades Publishing, Inc., 2013.
Original Russian Text © V.I. Zinenko, M.S. Pavlovskii, A.S. Krylov, I.A. Gudim, E.V. Eremin, 2013, published in Zhurnal Eksperimental'noi i Teoreticheskoi Fiziki, 2013, Vol. 144, No. 6, pp. 1174–1183.

SOLIDS AND LIQUIDS

Vibrational Spectra and Elastic, Piezoelectric, and Magnetoelectric Properties of $HoFe_3(BO_3)_4$ and $HoAl_3(BO_3)_4$ Crystals

V. I. Zinenko*, M. S. Pavlovskii, A. S. Krylov, I. A. Gudim, and E. V. Eremin

Kirensky Institute of Physics, Siberian Branch, Russian Academy of Sciences, Krasnoyarsk, 660036 Russia

**e-mail: zvi@iph.krasn.ru*

Received June 21, 2013

Abstract—Raman spectra of light are obtained for $HoFe_3(BO_3)_4$ and $HoAl_3(BO_3)_4$ crystals at various temperatures and are used for determining the frequencies of crystal lattice vibrations at the center of the Brillouin zone. It is also found that the $HoFe_3(BO_3)_4$ crystal exhibits a phase transition at $T_c \approx 366$ K. The magnetoelectric effect in the paramagnetic phase of these compounds is studied experimentally. The lattice vibration frequencies, elastic and piezoelectric moduli, Born dynamic charges, and the high-frequency permittivity are calculated using the density functional method. A peculiar behavior of the transverse acoustic vibration branch is observed in the $\Gamma \longrightarrow Z$ direction of the Brillouin zone of the $HoFe_3(BO_3)_4$ crystal. The electric polarization induced by an external field is estimated using the calculated values of piezoelectric moduli and experimental values of magnetostriction.

DOI: 10.1134/S1063776113140203

1. INTRODUCTION

The family of $RM_3(BO_3)_4$ crystals (R stands for a rare-earth ion and M = Al, Sc, Fe, Ga) has been actively studied in recent years owing to their interesting physical properties and their variety for various combinations of R and M elements. A crystal structure with the $R32$ space symmetry group and with a single molecule in the unit cell belongs to the structural type of natural mineral chantite [1]. The unit cell parameters and relative coordinates of atoms are given in Table 1. Depending on their chemical composition, upon a change in temperature some crystals of this family exhibit a peculiar phase transition $R32 \longrightarrow P3_121$, in which only the translational symmetry of the crystal changes. Point symmetry D_3 is preserved in this transition. $RFe_3(BO_3)_4$ compounds experience a phase transition from the paramagnetic to the antiferromagnetic state. The magnetic properties of ferroborates were discussed in detail in reviews [3, 4].

In recent years, the emergence of electric polarization was observed in this family of crystals as a result of transition to the antiferromagnetic state [4] (the authors of [4] called this polarization "spontaneous") or under the action of an external magnetic field applied to the crystal [5]. In particular, the behavior of polarization in $HoFe_3(BO_3)_4$ compound below the Néel temperature was studied in [4]; in [5], the emergence of polarization and its dependence on the applied magnetic field was detected in a fairly wide temperature range in $HoAl_3(BO_3)_4$, which exhibits no magnetic ordering down to very low temperatures. It should be noted that the value of electric polarization

Table 1. Lattice parameters and relative coordinates of atoms in $HoFe_3(BO_3)_4$ [1] and $HoAl_3(BO_3)_4$ [2] crystals in the $R32$ phase

		Fe	Al
a, Å		9.5337	9.2900
c, Å		7.5711	7.231
Ho (3*a*)	*x*	0	0
	y	0	0
	z	0	0
M (9*d*)	*x*	0.4508	0.44333
	y	0	0
	z	0	0
B1 (3*b*)	*x*	0	0
	y	0	0
	z	1/2	1/2
B2 (9*e*)	*x*	0.55070	0.55836
	y	0	0
	z	1/2	1/2
O1 (9*e*)	*x*	0.1446	0.14947
	y	0	0
	z	1/2	1/2
O2 (9*e*)	*x*	0.4074	0.40883
	y	0	0
	z	1/2	1/2
O3 (9*e*)	*x*	0.5444	0.55053
	y	0.8531	0.85035
	z	0.4842*	0.47802

The asterisk marks the free coordinate, which was varied in calculations (see text).

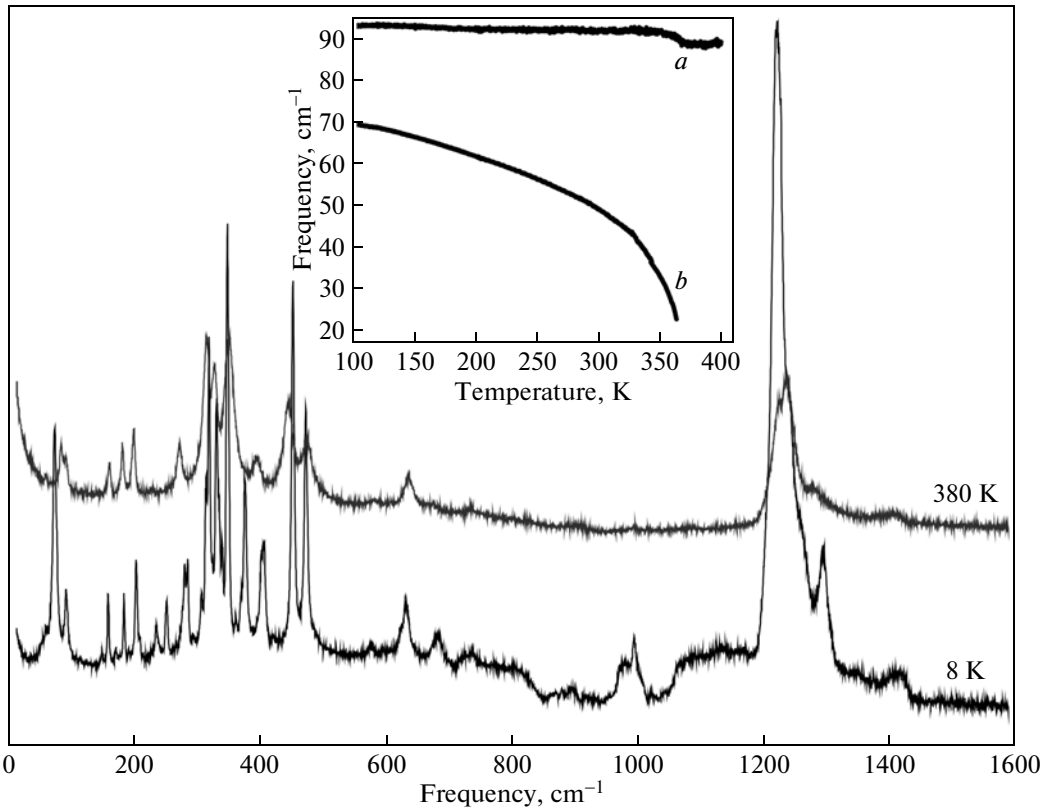

Fig. 1. Raman spectra of the $HoFe_3(BO_3)_4$ crystal at $T = 380$ and 8 K. The inset shows the positions of the lines depending on the temperature for the hard mode (*a*) and soft mode (*b*) during the structural phase transition.

induced by the magnetic field in $HoAl_3(BO_3)_4$ is two orders of magnitude higher than the "spontaneous" polarization in $HoFe_3(BO_3)_4$ [4, 5]. The experimental phonon spectra and elastic properties of some representatives of the $RM_3(BO_3)_4$ family were studied in [6–8]. For the $HoFe_3(BO_3)_4$ and $HoAl_3(BO_3)_4$ crystals considered here, we have found no information on the vibrational spectra and elastic properties in the literature.

This study aims at experimentally determining the limiting vibrational frequencies for $HoFe_3(BO_3)_4$ and $HoAl_3(BO_3)_4$ crystals, measuring the electric polarization induced by an external magnetic field in the paramagnetic phase of the $HoFe_3(BO_3)_4$ and $HoAl_3(BO_3)_4$ crystals, and estimating the magnetoelectric effect using the calculated values of the piezoelectric moduli and experimental values of magnetostriction constants for the crystals under investigation.

2. EXPERIMENTAL RESULTS

$HoFe_3(BO_3)_4$ and $HoAl_3(BO_3)_4$ single crystals were grown from a solution–melt in accordance with the technique described in [9] and were up to 5 mm in size. The samples were oriented using the X-ray method. The polarization spectra of Raman scattering of light were analyzed in the temperature range 8–400 K on a T64000 spectrometer under pumping with radiation from an argon laser with wavelengths of 514 nm ($HoFe_3(BO_3)_4$) and 488 nm ($HoAl_3(BO_3)_4$). The experimental spectra for these compounds are shown in Figs. 1 and 2 for two values of temperature (8 and 380 K for $HoFe_3(BO_3)_4$ and 8 and 300 K for $HoAl_3(BO_3)_4$). It can be seen that in the case of the $HoAl_3(BO_3)_4$ crystal, the lattice vibration spectra at higher and lower temperatures differ insignificantly (at any rate, no additional vibrational frequencies appear at the low temperature), while the vibrational spectrum for $HoFe_3(BO_3)_4$ at the lower temperature differs significantly from its spectrum at 380 K. It can be seen from Fig. 1 that the spectrum of $HoFe_3(BO_3)_4$ at $T <$ 380 K acquires new vibrational modes indicating the structural phase transition in this compound, which was observed earlier in heat capacity measurements [10]. Analysis of the temperature dependence of the soft mode in the $P3_121$ phase (see inset to Fig. 1) gives a temperature of $T_c \approx 366$ K for the structural phase transition $P32 \longrightarrow P3_121$. The temperature of this transition determined in [10] was 427 K. The reason for such a strong difference in the values of the phase-transition temperature determined from the phonon spectra and from the specific heat for the $HoFe_3(BO_3)_4$ compound remains unclear.

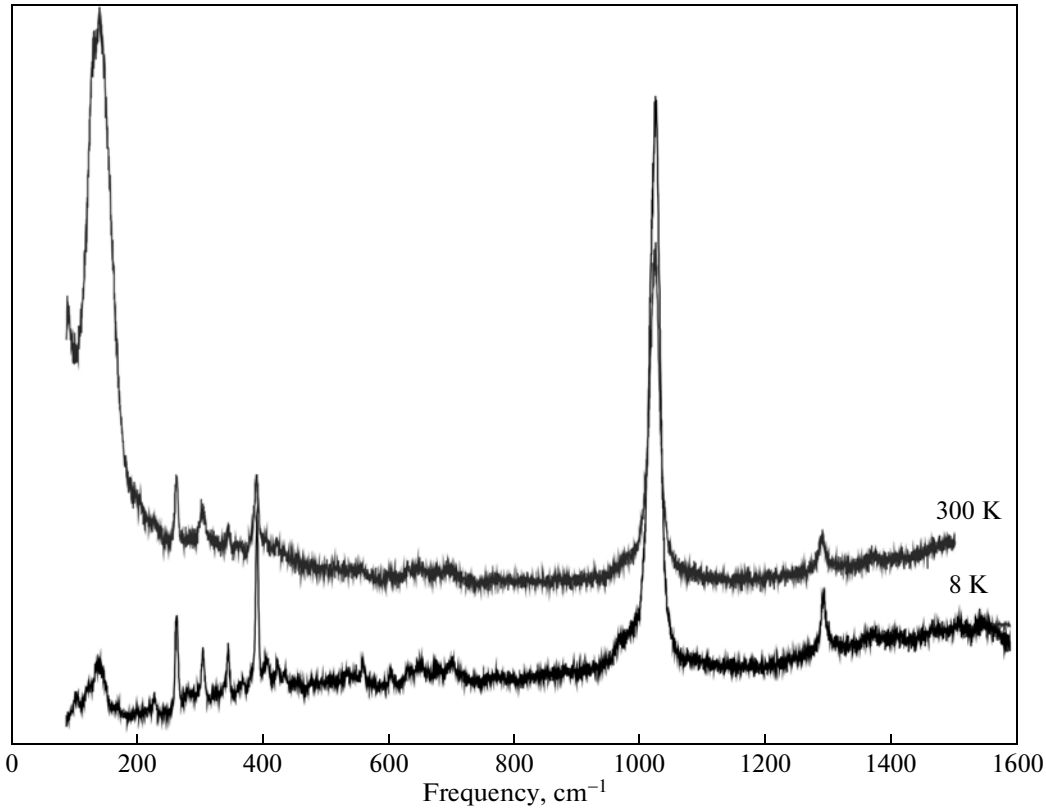

Fig. 2. Raman spectra of the $HoAl_3(BO_3)_4$ crystal at $T = 300$ and 8 K.

It should be noted that the spectra of these compounds are qualitatively similar to the spectra of other rare-earth borates for which such spectra are known [6].

Table 2 contains the experimental values of the active vibrational frequencies in the Raman spectra of compounds $HoFe_3(BO_3)_4$ and $HoAl_3(BO_3)_4$ in comparison with the results of calculations described in Section 3.

The magnetoelectric studies were carried out by measuring the charge between two contacts (deposited using an epoxy resin with a conducting filler) on the opposite sides of a plane-parallel plate with the help of the Keithley 6517B electrometer. The temperature and the magnetic field were controlled by PPMS-9 (Quantum Design).

Figure 3 shows the field dependences $\Delta P_{bb}(H_b)$ of the longitudinal electric polarization of $HoFe_3(BO_3)_4$ and $HoAl_3(BO_3)_4$ recorded at various temperatures. The dependences for $HoAl_3(BO_3)_4$ coincide qualitatively with those obtained in [5] in the *ab* direction (the electric polarization is recorded along direction *a* and magnetic field is applied along direction *b*) and coincide quantitatively with the dependences obtained earlier [11] for the same direction.

3. RESULTS OF CALCULATING THE VIBRATIONAL SPECTRUM OF THE CRYSTAL LATTICE AND THE ELASTIC AND PIEZOELECTRIC MODULI

The crystal lattice dynamics, high-frequency permittivity tensor components, Born dynamic charges, and elastic and piezoelectric moduli for the $HoFe_3(BO_3)_4$ and $HoAl_3(BO_3)_4$ crystals are calculated using a nonempirical model of polarizable ions. The details of this model are described in [12]. All calculations are carried out using the experimental values of the lattice parameters and atomic coordinates given in Table 1. Table 2 contains the values of vibrational frequencies at the center of the Brillouin zone for $HoFe_3(BO_3)_4$ and $HoAl_3(BO_3)_4$ in the rhombohedral phase in comparison with the experimental values. The decomposition of the vibrational representation in terms of irreducible representations has the form $\Gamma = 7A1 + 13A2 + 20E$, including acoustic modes $A2 + E$. The $A1$-type modes are active in the Raman spectra, $A2$-type modes are active in the IR spectra, and doubly degenerate E-type modes are active in the Raman and IR spectra. It follows from Table 2 that the limiting vibrational frequencies for both compounds under investigation in the range of low (no more than 200 cm^{-1}) and high frequencies (about 1100–

Table 2. Limiting vibrational frequencies (cm^{-1}) of $HoFe_3(BO_3)_4$ and $HoAl_3(BO_3)_4$ crystals in the $R32$ phase

Experiment		Calculation			Experiment		Calculation		
$HoFe_3(BO_3)_4$		$HoFe_3(BO_3)_4$			$HoAl_3(BO_3)_4$		$HoAl_3(BO_3)_4$		
$A1$	E	$A1$	$A2$	E	$A1$	E	$A1$	$A2$	E
181	84	133	72	64	259	115	193	62	64
315	160	261	127	125	301	402	279	80	157
474	199	353	129	159	525	553	332	152	183
634	229	494	201	182	768	625	497	187	200
995	271	820	205	202	888	972	780	216	212
1237	327	852	217	219	1201	923	827	222	244
	351	1253	248	243		956	1159	240	250
	392		261	255		1023		265	267
	446		479	285		1169		450	276
	580		578	302		1166		527	298
	675		652	321		1294		630	313
	737		1292	461				1307	446
	910			468					454
	1405			491					475
				645					627
				847					811
				1201					1112
				1245					1162
				1311					1331

1400 cm^{-1}) are in satisfactory agreement with experimental values, while the conformity between the calculated and experimental values of vibrational frequencies in the medium frequency range (200–1000 cm^{-1}) is less satisfactory.

Table 3 contains the calculated values of the high-frequency permittivity tensor component and Born dynamic charges. It can be seen from the table that the Born dynamic charge tensor Z_{ik} for Ho and Fe(Al) is almost isotropic, while the Z_{ik} components for boron and oxygen ions exhibit strong anisotropy. In particular, the value of the Z_{zz} component for boron ions, which is related to boron vibrations in the direction perpendicular to the plane of the BO_3 triangle, is anomalously small. Unfortunately, we failed to find experimental or calculated data on dynamic charges for crystals of this family in the literature. As regards components ε_∞, we have found no experimental data on the refractive indices for the compounds considered here; however, the values of ε_{xx}, ε_{yy}, and ε_{zz} given in Table 3 are in satisfactory agreement with the corresponding values, for example, for crystal $LaSc_3(BO_3)_4$ belonging to the same family, for which $\varepsilon_{xx} = \varepsilon_{yy} = 3.35$ and $\varepsilon_{zz} = 3.06$ [13].

Figures 4 and 5 show a part of the lattice vibration spectra (in directions $\Gamma \longrightarrow Z \longrightarrow A \longrightarrow Z' \longrightarrow X \longrightarrow \Gamma$ of the Brillouin zone, where $Z = 1/2\ (\mathbf{b}_1 + \mathbf{b}_2 + \mathbf{b}_3)$, $A = 1/2\mathbf{b}_1$, $Z' = 1/2\ (\mathbf{b}_1 - \mathbf{b}_2 - \mathbf{b}_3)$, and $X = 1/2\ (\mathbf{b}_1 - \mathbf{b}_3)$, $\mathbf{b}_1$, $\mathbf{b}_2$, and $\mathbf{b}_3$ being the reciprocal lattice vectors in the rhombohedral setup) of the $HoFe_3(BO_3)_4$ and $HoAl_3(BO_3)_4$ crystals in the structure with the $R32$ space symmetry group, which were calculated from the experimental values of the unit cell parameters and atomic coordinates (see Table 1).

The $HoFe_3(BO_3)_4$ crystal exhibits the structural phase transition $R32\ (n = 1) \longrightarrow P3_121\ (n = 3)$ (n is the number of molecules in the unit cell), in which only

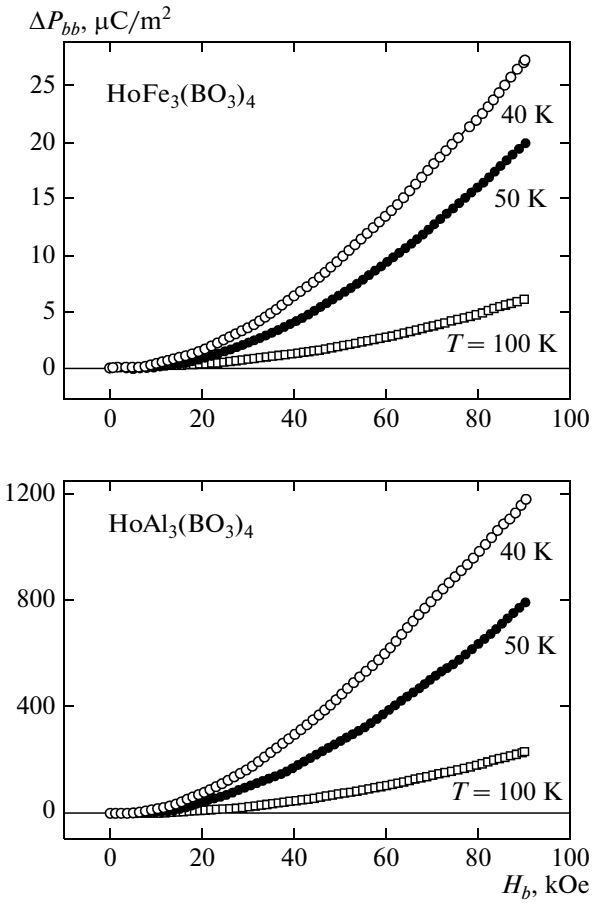

Fig. 3. Dependence of longitudinal electric polarization ΔP_{bb} on applied magnetic field H_b at various temperatures for $HoFe_3(BO_3)_4$ and $HoAl_3(BO_3)_4$ crystals.

the translational symmetry of the crystals changes. According to the available data, the temperature of this phase transition is $T = 427$ K [10]; according to the data considered in Section 2, this transition occurs at $T_c \approx 366$ K. It can be seen from Figs. 4 and 5 that the vibrational spectra of $HoFe_3(BO_3)_4$ and $HoAl_3(BO_3)_4$ calculated from the experimental values of atomic coordinates contain no unstable modes. However, our calculations show that the behavior of one of the transverse acoustic vibration branches with wavevector $\lambda = \mu(\mathbf{b}_1 + \mathbf{b}_2 + \mathbf{b}_3)$ ($0 \le \mu \le 1/2$) is very sensitive to the value of free coordinate z of the O3 oxygen ion (this coordinate is marked by asterisk in Table 1).

Figure 6 shows the behavior of the λ_3 branch (double acoustic mode at the center of the Brillouin zone splits into two single modes $E = \lambda_2 + \lambda_3$) for several values of free coordinate z of the O3 ion. The same figure shows for comparison the behavior of two acoustic branches λ_1 and λ_2. It follows from Fig. 6 that longitudinal λ_1 branch and one of the transverse acoustic branches (λ_2) are almost insensitive to the variation of coordinate z; at the same time, upon a change in coordinate z of oxygen O3, anomaly is observed in the dispersion relation for mode λ_3 (namely, the vibrational frequencies of this mode tend to zero upon an increase in z in the range of wavevector $q = 1/3\ (\mathbf{b}_1 + \mathbf{b}_2 + \mathbf{b}_3)$). Table 4 shows a part of the eigenvector (because of the lack of space, only the ions of holmium and iron are shown) of the mode λ_3 ($q = 1/3\ (\mathbf{b}_1 + \mathbf{b}_2 + \mathbf{b}_3)$). The distortion in the $R32$ phase in this eigenvector leads to space group $P3_121$ with three molecules in the unit cell, which corresponds to the experimentally observed structure below T_c in some rare-earth ferroborates (in particular, in $HoFe_3(BO_3)_4$ [1]) and is in agreement with the results of the group-theoretical analysis (see, for example, ISOTROPY program [14]), according to which the phase transition $R32\ (n = 1) \longrightarrow P3_121\ (n = 3)$ is associated with one component of the 2D complete representation Λ_3 (the asterisk of representation Λ_3 contains two vectors $q_1 = \mu(\mathbf{b}_1 + \mathbf{b}_2 + \mathbf{b}_3)$ and $q_2 = -\mu(\mathbf{b}_1 + \mathbf{b}_2 + \mathbf{b}_3)$ [15]).

Table 3. Born dynamic charge tensor components in the units of the electron charge and high-frequency permittivity of $HoFe_3(BO_3)_4$ and $HoAl_3(BO_3)_4$ crystals in the *R*32 phase

	$HoFe_3(BO_3)_4$			$HoAl_3(BO_3)_4$		
	Z_{ik} ($i = x, y, z$; $k = x, y, z$)			Z_{ik} ($i = x, y, z$; $k = x, y, z$)		
Ho	3.37	0	0	3.39	0	0
	0	3.36	−0.03	0	3.39	−0.03
	0	0.01	3.27	0	0	3.28
Fe/Al	3.47	−0.05	0.03	3.51	−0.11	0.07
	0.01	3.49	0.15	−0.03	3.60	0.11
	0.01	0.01	3.89	0	0	3.47
B1	4.20	0	0	4.14	0	0
	0	4.25	−0.05	0	4.16	−0.05
	0	0.02	0.74	0	0	0.93
B2	3.52	−0.32	0.08	3.50	−0.34	0.28
	−0.21	3.90	0.01	−0.23	3.87	0.14
	0.29	0.20	1.05	0.30	0.19	1.23
O1	−2.11	1.07	−0.48	−2.03	1.16	−0.46
	1.01	−3.10	−0.30	1.17	−3.16	−0.30
	−0.32	−0.21	−1.59	−0.26	−0.16	−1.57
O2	−1.99	1.17	−0.38	−1.96	1.28	−0.41
	1.20	−3.31	−0.22	1.32	−3.35	−0.22
	−0.30	−0.18	−1.48	−0.24	−0.14	−1.40
O3	−1.69	−0.66	−0.07	−1.68	−0.82	−0.21
	−0.96	−2.76	−0.59	−1.03	−2.79	−0.68
	−0.18	−0.51	−1.62	−0.21	−0.47	−1.57
	ε_{xx}	ε_{yy}	ε_{zz}	ε_{xx}	ε_{yy}	ε_{zz}
ε	4.05	4.05	2.93	4.30	4.30	3.04

In this calculation, the squared frequency of the λ_3 mode ($q = 1/3$ ($\mathbf{b}_1 + \mathbf{b}_2 + \mathbf{b}_3$)) becomes negative in the case of considerable distortion of the experimentally determined structure in the *R*32 phase (the value of the *z* coordinate for oxygen O3 is ≈0.53; this corresponds to a displacement of oxygen O3 from the experimentally determined position by approximately 0.3 Å, which is unlikely). Therefore, from the results of this calculation, we can judge only about the qualitative behavior of the unstable vibrational mode λ_3. It should be noted in this connection that in accordance with the results of our calculations, the dipole and quadrupole interactions taken into account in the model used here stabilize the λ_3 mode: disregarding these interactions (rigid ion model), the anomalous dispersion relation for the λ_3 mode is more sensitive to the value of the *z* coordinate of oxygen O3, as shown in Fig. 7.

The results of calculating the elastic and piezoelectric moduli of $HoFe_3(BO_3)_4$ and $HoAl_3(BO_3)_4$ are given in Table 5. Unfortunately, we have found no experimental data on the elastic properties of these compounds; however, we can compare our values of the elastic constants with the experimental data available for other crystals from this family (in particular,

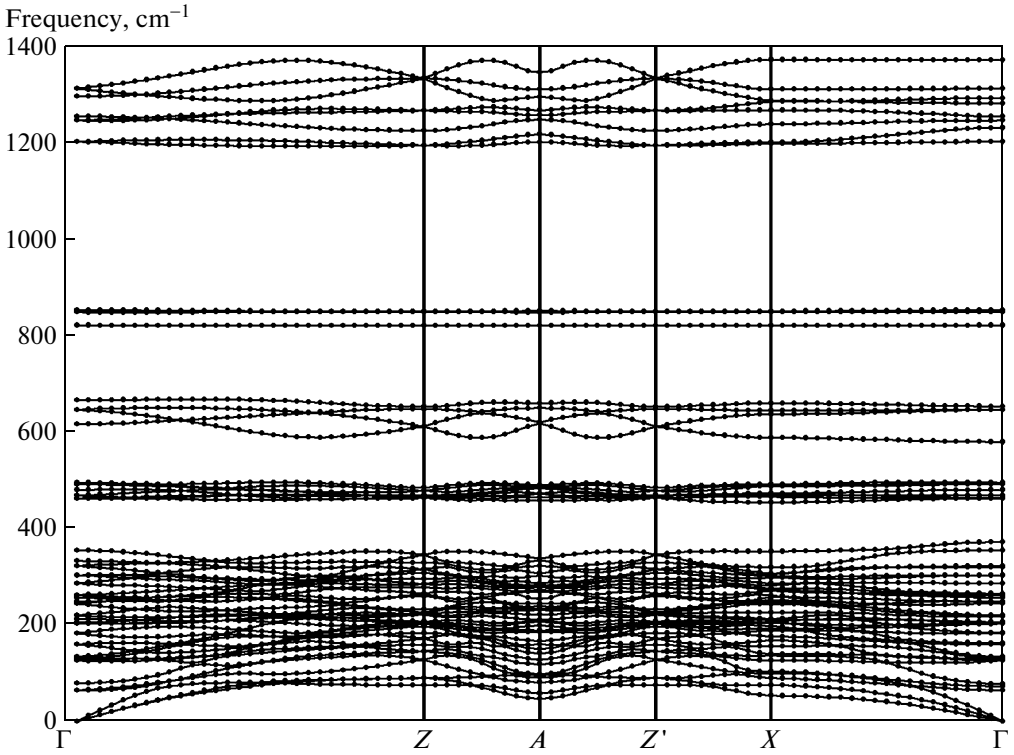

Fig. 4. Calculated phonon spectrum of the $HoFe_3(BO_3)_4$ crystal.

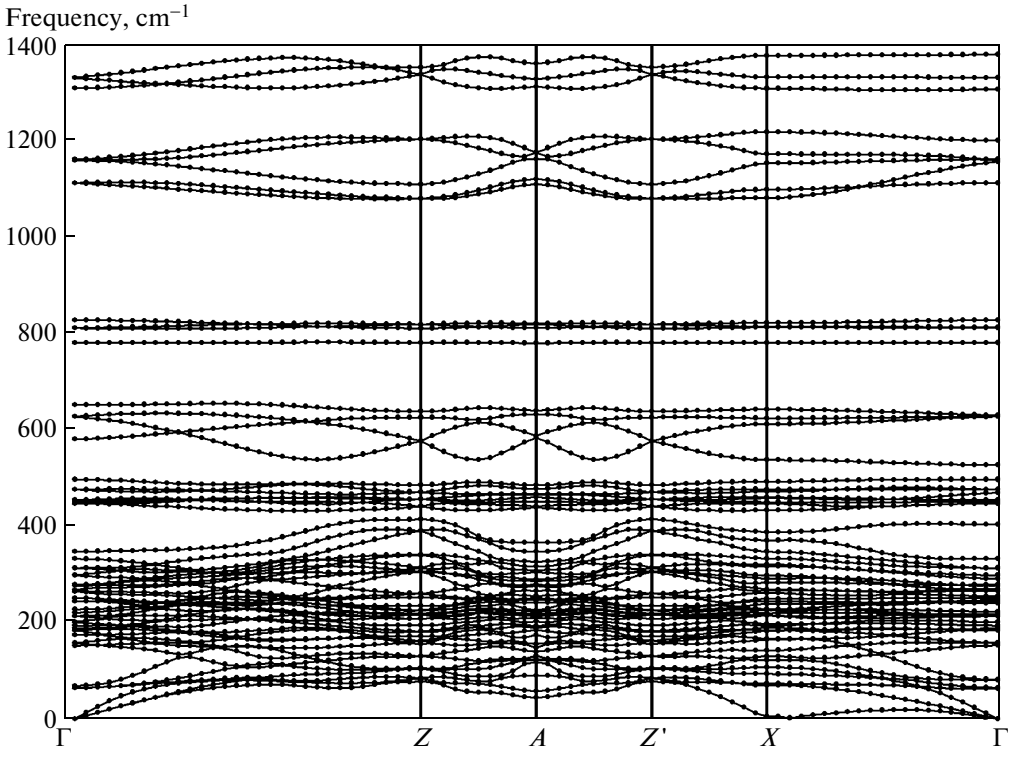

Fig. 5. Calculated phonon spectrum of the $HoAl_3(BO_3)_4$ crystal.

crystal induces polarization $P_k = e_{ki}u_i$, where e_{ki} is the tensor of piezoelectric moduli. Consequently, as a result of application of external magnetic field to the paramagnetic phase of the crystal, electric polarization $P \propto H^2$ appears in it (this dependence is indeed observed as can be seen from Fig. 3). To estimate the polarization induced by the magnetic field in these crystals, we will use the calculated piezoelectric moduli values (see Table 5) and experimental data on magnetoelastic coupling. For the $HoAl_3(BO_3)_4$ crystal, we used the value of magnetostriction obtained in [5] (8×10^{-5}). For the $HoFe_3(BO_3)_4$ crystal, we could not find measurement magnetostriction results in the literature; for this reason, we estimated the polarization in this crystal using the value 5×10^{-6} obtained in [17] for the magnetostriction of the $GdFe_3(BO_3)_4$ crystal. The values of polarization calculated here for the $HoFe_3(BO_3)_4$ and $HoAl_3(BO_3)_4$ crystals were 4.95 and 140 $\mu C/m^2$, respectively; the experimental values of the polarization of the $HoFe_3(BO_3)_4$ and $HoAl_3(BO_3)_4$ crystal obtained in this study were 40 and 1200 $\mu C/m^2$, respectively.

4. CONCLUSIONS

Let us briefly list the results of this study.

(1) We measured the Raman spectra in the $HoFe_3(BO_3)_4$ and $HoAl_3(BO_3)_4$ crystals and performed nonempirical calculation of the vibrational spectra of the crystal lattice, Born dynamic charges, and elastic and piezoelectric moduli. The limiting vibrational frequencies are in satisfactory agreement with the measured values.

(2) We found as a result of calculations that the experimental values of the unit cell parameters and the atomic coordinates in the vibrational spectra of the crystal lattice do not indicate the presence of an unstable vibrational mode. We showed, however, that the vibrational frequencies of the transverse acoustic branch in the $\Gamma \longrightarrow Z$ direction of the Brillouin zone are very sensitive to the value of free coordinate z of oxygen O3; for a certain value of z (as noted in Section 3, the calculated value is hardly feasible), the vibrational frequency of the lattice for $q \approx 1/3(\mathbf{b}_1 + \mathbf{b}_2 + \mathbf{b}_3)$ becomes imaginary. Unfortunately, we are aware of no experimental phonon spectra for crystals of the given family; analysis of the dispersion of the transverse acoustic branch in direction $\Gamma \longrightarrow Z$ would be of undoubted interest. This instability of the crystal lattice is associated with the structural phase transition $R32$ ($n = 1$) $\longrightarrow$ $P3_121$ ($n = 3$), which is observed in the $HoFe_3(BO_3)_4$ crystal and in some other crystals of this family.

(3) We studied experimentally the magnetoelectric effect in the paramagnetic phase of the $HoFe_3(BO_3)_4$ and $HoAl_3(BO_3)_4$ crystals and demonstrated that the electric polarization induced by an external magnetic field in the aluminum-based compound is 30 times as high as the polarization in the iron-based compound in the same magnetic field. The polarization induced by the external magnetic field is estimated using the calculated values of piezoelectric moduli and from the available experimental data on magnetostriction. The values obtained for the polarization of these two compounds are about an order of magnitude lower than the experimental values; however, these estimates show that the polarization in the $HoAl_3(BO_3)_4$ compound is 30 times as high as the same value for $HoFe_3(BO_3)_4$ in accordance with the experimental data, and this difference is mainly due to the difference in the values of magnetostriction in these compounds.

ACKNOWLEDGMENTS

This study was supported financially by the President of the Russian Federation under the program "Leading Scientific Schools" (grant no. NSh 4828.12.2), the Russian Foundation for Basic Research (project no. 12-02-00025-a), and the Ministry of Education and Science of the Russian Federation (contract no. 8365).

REFERENCES

1. C. Ritter, A. Vorotynov, A. Pankrats, G. Petrakovskii, V. Temerov, I. Gudim, and R, Szymczak, J. Phys.: Condens. Matter **20** (36), 365209 (2008).

2. M. S. Molokeev, personal communication.

3. A. N. Vasiliev and E. A. Popova, Low Temp. Phys. **32**(8–9), 735 (2006).

4. A. M. Kadomtseva, Yu. F. Popov, G. P. Vorob'ev, A. P. Pyatakov, S. S. Krotov, K. I. Kamilov, V. Yu. Ivanov, A. A. Mukhin, A. K. Zvezdin, A. M. Kuz'menko, L. N. Bezmaternykh, I. A. Gudim, and V. L. Temerov, Low Temp. Phys. **36** (6), 511 (2010).

5. K.-C. Liang, R. P. Chaudhury, B. Lorenz, Y. Y. Sun, L. N. Bezmaternykh, V. L. Temerov, and C. W. Chu, Phys. Rev. B: Condens. Matter **83** (18), 180417(R) (2011).

6. D. Fausti, A. A. Nugroho, P. H. M. van Loosdrecht, S. A. Klimin, M. N. Popova, and L. N. Bezmaternykh, Phys. Rev. B: Condens. Matter **74** (2), 024403 (2006).

7. G. A. Zvyagina, K. R. Zhekov, L. N. Bezmaternykh, I. A. Gudim, I. V. Bilych, and A. A. Zvyagin, Low Temp. Phys. **34** (11), 901 (2008).

8. G. A. Zvyagina, K. R. Zhekov, I. V. Bilych, A. A. Zvyagin, L. N. Bezmaternyhk, and I. A. Gudim, Low Temp. Phys. **36** (4), 296 (2010).
9. L. N. Bezmaternykh, V. L. Temerov, I. A. Gudim, and N. A. Stolbovaya, Crystallogr. Rep. **50** (Suppl. 1), S97 (2005).
10. Y. Hinatsu, Y. Doi, K. Ito, M. Wakeshima, and A. Alemi, J. Solid State Chem. **172** (2), 438 (2003).
11. A. I. Begunov, A. A. Demidov, I. A. Gudim, and V. E. Eremin, JETP Lett. **97** (9), 528 (2013).
12. E. G. Maksimov, V. I. Zinenko, and N. G. Zamkova, Phys.—Usp. **47** (11), 1075 (2004).
13. J. Cho, S. Lee, and Y. M. Yu, J. Korean Phys. Soc. **50**, 1090 (2007).
14. H. T. Stokes, D. M. Hatch, and B. J. Campbell, ISOTROPY (2007). http://stokes.byu.edu/isotropy.html.
15. O. V. Kovalev, *Irreducible and Induced Representations and Co-Representations of Fedorov Groups* (Nauka, Moscow, 1986) [in Russian].
16. B. P. Sorokin, D. A. Glushkov, A. V. Kodyakov, L. N. Bezmaternych, V. L. Temerov, and I. A. Gudim, Vestn. Krasn. Gos. Univ., No. 5, 49 (2004).
17. A. M. Kadomtseva, Yu. F. Popov, S. S. Krotov, G. P. Vorob'ev, E. A. Popova, A. K. Zvezdin, and L. N. Bezmaternykh, Low Temp. Phys. **31** (8–9), 807 (2005).

Translated by N. Wadhwa